Histol Histopathol (2020) 35: 47-56

http://www.hh.um.es

Histology and Histopathology
From Cell Biology to Tissue Engineering

Morphological changes during the formation of amoebic liver abscess in vagotomized hamsters

Esperanza Sánchez-Alemán[1], Leticia María Lili-Carrillo[2], Martin Humberto Muñoz-Ortega[3], Ma. Consolación Martínez-Saldaña[1] and Javier Ventura-Juárez[1]

[1]Departamento de Morfología, Universidad Autónoma de Aguascalientes, Aguascalientes, [2]Instituto Politécnico Nacional Centro Interdisciplinario de Ciencias Marinas, Biología Marina y Pesquerías, La Paz, Baja California Sur and [3]Departamento de Química, Universidad Autónoma de Aguascalientes, Aguascalientes, México

Summary. Amoebic liver abscess (ALA) is the main extra-intestinal complication caused by *Entamoeba histolytica*. Given the histological features of ALA in hamsters and the importance of the vagus nerve in the immune response, the aim of this study was to identify and analyze the major changes in ALA that are caused by a vagotomy. The changes found are related to inflammatory foci and abscess size, the type of collagen formed, and the number of trophozoites in lesions. Male hamsters were divided into three groups: Intact animals (IA) and those undergoing a false operation (SHAM) or a subdiaphragmatic vagotomy (VAG). In each group, *E. histolytica* trophozoites or culture medium (CM) were inoculated in hamsters by the intrahepatic route, and then euthanized at 6h, 12h, 24h, 48h, 4d or 7d post-infection. Initially the growth of the abscess was more rapid in the VAG group, but at day 7 it was faster in the IA and SHAM groups. VAG animals showed a higher quantity of type III collagen than the IA and SHAM groups. A larger number of amoebic trophozoites/mm^2 was observed up to day 4 in VAG hamsters (23.3±2.19) compared to IA (14.6±0.23) and SHAM (6.13±0.87) animals. This parameter decreased by day 7 in VAG (13.4±0.87) with respect to IA (24.7±1.47) and SHAM (21.7±1.48). The results show that a subdiaphragmatic vagotomy influenced the development of ALA in hamsters, suggesting a modification of the morphological structure of damaged hepatic tissue.

Offprint requests to: Javier Ventura-Juárez PhD, Avenida Universidad 940, Colonia Ciudad Universitaria, Edificio 202, Aguascalientes, 20131-México. e-mail: jventur@correo.uaa.mx or esanchezal@hotmail.com
DOI: 10.14670/HH-18-134

Key words: Vagotomy, Liver morphology, Amoebic liver abscess, Collagen

Introduction

Amoebiasis is a disease caused by the *Entamoeba histolytica* protozoan (amoebae or trophozoites) that affects the human intestine. It is considered the third leading cause of death from parasitic diseases, surpassed only by malaria and schistosomiasis (Davis and Pawlowski, 1985).

The main form of extra-intestinal infection is amoebic liver abscess (ALA), which can develop serious complications if not diagnosed correctly (Salles et al., 2003). From the clinical point of view, the symptoms of ALA (e.g., fever and right upper quadrant pain) can be confused with many disorders, including acute cholecystitis, perforated peptic ulcer, acute hepatitis, cirrhosis, hydatid cysts, pancreatic pseudocysts, pneumonia, acute pleurisy with effusion, empyema, chronic lung disease, tuberculosis and fever of unknown origin (Mukhopadhyay et al., 2010).

Previous reports have characterized ALA in regard to its morphology, with its principal cells involved in acute phase like endothelial, neutrophils and macrophages (Ventura-Juarez et al., 2002), complications (such as lung abscess and pericarditis), and possible treatments (Rogers, 1922; Mullan and Williams, 1965). Tissue destruction appears to be the basis of this disease (Petri et al., 2002). The spread of amoebae leads to the formation of small abscesses that in some cases can cause obstruction in the portal vein

and bile duct, leading to portal hypertension and jaundice (Aikat et al., 1979). *In vitro* studies have shown that the trophozoites are capable of lysing a variety of host cells, including hepatocytes, intestinal epithelial cells, neutrophils, lymphocytes and macrophages. The pathology of ALA is characterized by areas of necrosis, with the possible formation of cavities filled with cellular debris (Ragland et al., 1994).

By using the model of ALA in hamsters (susceptible model) and an intraportal inoculation of trophozoites, the various stages of development have been categorized, from the early hours up to 7 days post-inoculation. The malady begins with small scattered inflammatory foci and expands to large granulomas that can become abscesses with necrotic areas surrounded by *E. histolytica* trophozoites (Tsutsumi et al., 1984; Ventura-Juarez et al., 2002).

Neuroimmune regulation plays an important role during the development of the disease because it balances and integrates the immune response to pathogens and damaged tissue (Otmishi et al., 2008). The vagus nerve (VN) serves as the main parasympathetic innervation route for thoracic and abdominopelvic viscera as well as their main neurotransmitter, acetylcholine (nACh). By traveling through this pathway, nACh decreases proinflammatory cytokine expression by binding to the acetylcholine α7 nicotinic receptor (nAChRa7), expressed primarily in macrophages and other cells of the immune response (Borovikova et al., 2000; Henry, 2002; Wang et al., 2003).

In hamsters, inhibition of the parasympathetic nervous system has induced histological changes as well as differences in the production of pro- and anti-inflammatory cytokines, immune cell location, and distribution of collagen. Although these changes have been observed in ALA granulomas after 7 days of development (Munoz-Ortega et al., 2011; Sanchez-Aleman et al., 2015), there has not yet been any report, to our knowledge, about the histological changes, tissue damage, and distribution of *E. histolytica* trophozoites in liver tissue during the complete evolution of ALA from the arrival of amoebae to this organ to the 7th day of development.

The aim of this study was to explore the effect that the absence of vagus nerve may have on tissue structure and other aspects of the development of ALA from 6 h to 7 d post-inoculation. For this purpose, we comparatively describe the morphological development of ALA in control hamsters (intact and sham-operated) and those having undergone a subdiaphragmatic vagotomy.

Materials and methods

Animal model and experimental design

One hundred and eight male golden hamsters (*Mesocricetus auratus*) aged 6-8 weeks and weighing 100-150 g were previously treated with metronidazole (7.5 mg/kg for 5 days) to eliminate intestinal parasites. The use of these animals was previously approved, and they were treated according to the rules of the Bioethics Commission of the Autonomous University of Aguascalientes, and the NIH guide for animal research (Guide for the care and Use of Laboratory Animals, 2002). The hamsters were divided into three groups (n=36): intact (IA) and sham-operated (SHAM) animals, and those that underwent a subdiaphragmatic vagotomy (VAG) to disable the parasympathetic nervous system in the liver.

Vagotomy and amoebic liver abscess (ALA) induction

After 24 h of fasting and under anesthesia (pentobarbital 25-40 mg/kg), animals in the SHAM and VAG groups underwent surgical dissection using microsurgery method with the help of the stereoscope equipment. For VAG animals, the liver and intestinal vagal branches were dissected and sliced. The subdiaphragmatic vagal branches were identified, then dissected up to the esophagus and the liver; For the SHAM animals, the hepatic and intestinal branches of the VN were gently manipulated but not cut (Tanaka et al., 1987).

At 30 days post-surgery, the process of inducing ALA began by intrahepatic inoculation of *E. histolytica* trophozoites HM1:IMSS. The amoebae were axenically cultivated in BI-S-33 medium + 15% (v/v) bovine adult serum (Microlab SU-120) that was inactivated at 56°C for 30 minutes (Diamond et al., 1978). To maintain the virulent phase, amoebae were repetitively inoculated each two weeks into hamster livers. Half of the animal model of IA, SHAM and VAG were used for the control groups and injected with culture medium (CM) only. The animals were euthanized with an overdose of pentobarbital at 6 h, 12 h, 24 h, 2 d, 4 d or 7 d post-infection. To corroborate the efficacy of each subdiaphragmatic vagotomy, during the autopsy, the totality of the liver denervation was assessed; since gastric dilation is used as a sign of vagotomy, the stomach was removed and weighed (Sierra-Puente et al., 2009; Munoz-Ortega et al., 2011; Sanchez-Aleman et al., 2015).

ALA macroscopic evaluation: localization and in situ quantification of amoebae

After euthanasia, a comparison was made of the size, shape and development of abscesses in the liver of the different groups. Representative samples of inflammatory tissue and ALA were fixed in 4% paraformaldehyde, immersed in paraffin, and sliced at 5-μm. Slices were placed on microscope slides pretreated with 3-aminopropyl-triethoxy-silane (Sigma A3648 M. USA). The location of trophozoites and verification of infection was performed by immunohistochemistry with a lab-made anti *E. histolytica* (created in our laboratory) diluted at 1:500 (Ventura-Juárez et al., 2002). After

dewaxing the samples with xylene and rehydrating them, the epitopes were unmasked with 0.02 M citrate buffer at 120°C for 10 minutes.

For immunohistochemistry, the activity of the endogenous peroxidases was blocked with methanol-peroxide 1% at room temperature (RT) for one hour, and the unspecific reactions were blocked by treatment with fetal bovine serum at 10% in PBS at RT for 1 hour. The slices were incubated overnight at 4°C with the primary antibody and then incubated with the secondary antibody marked with peroxidase (Dako Envision Dual Link System-HRP K4061 Carpinteria, California USA). The reaction was completed by adding 3,3'-diamino-benzidine (D-8001; Sigma, USA) and H_2O_2 as a substrate for 1 min. The samples were counterstained with hematoxylin, dehydrated with alcohol, and mounted with high-speed inclusion medium (Entellan; Merck 64271, Germany) (Sanchez-Aleman et al., 2015). A count of amoebas in the hepatic tissue was made for each group (n=3) inoculated with *E. histolytica*. The microscopic inflammatory area was calculated using a morphometric technique with Image-Pro Plus software. Measurement of abscess size was performed macroscopically.

Hematoxylin-eosin, masson and sirius red staining

To evaluate the hepatic abscesses formed; Hematoxylin-eosin, Masson and Sirius Red Staining were performed for the liver tissues from ALA including AI, SHAM and VAG and the ones inoculated with CM. They were fixed with neutral formaldehyde by a histological technique. After being cleaned and dehydrated, the tissue samples were embedded in paraffin and cut in 5 μm slices, which were placed on slides. These tissue slices were then stained with hematoxylin & eosin (H&E) to evaluate the hepatic tissue and the histological structure of the abscesses formed, as well as the necrotic tissue, fibrosis and inflammatory infiltrate. To assess the healing of ALA lesions, Masson's trichrome stain was utilized to identify connective tissue in order to identify the intensity of the injury (e.g., collagen fibers) (Luna, 1968). After being deparaffinized with xylene, rehydrated with alcohol at different concentrations, and bathed in PBS, samples were incubated with a solution of picrosirius for 60 min (Junqueira et al., 1982; Montes and Junqueira, 1991; Schmitz et al., 2010). To identify distinct types of collagen, morphometric analysis was performed microscopically on the tissues of inflammatory and necrotic areas of ALAs, both in the central region and on the borders of the lesion. We used an Axioskop 4.0 microscope with a CoolSnap-Pro Digital photography system. Photographs were analyzed in Image-Pro Plus 4.5.0.19 Media Cybernetics.

Statistical analysis

The number of amoebae in the tissues from the different groups (those inoculated with *E. histolytica*) was compared by the Student's t test, followed by the ANOVA and post-hoc Tukey for comparisons of variance. All experiments were performed in triplicate. Data are presented as the mean±SD, with statistical significance considered at $p<0.05$. The Windows version of GraphPad Prism 6.01 was used for analysis.

Results

After the different post-inoculation development times for ALA from 6 h to 7 d, animals were euthanized and the liver was removed. The evolution of ALA could be observed for each of the three groups (IA, SHAM and VAG), with *E. histolytica* trophozoites. Considering the groups inoculated with *E. histolytica*, the progress of the abscesses was similar in the IA, SHAM and VAG hamsters, starting with small inflammatory foci at 6 h post-inoculation. At 12 h on (in the groups inoculated with *E. histolytica*), the increase in the size and aspect of the abscesses and the area of inflammation was similar in the IA (9.7±1.5 mm^2) and SHAM group, but the VAG group began to show differences (18.0±3.0 mm^2) ($p<0.05$). For 24 h it continued with a similar grown in IA (11.3±2.1 mm^2) and SHAM (13.5±2.3 mm^2) and with significant differences in VAG group (21.0±2.0 mm^2) ($p<0.05$) (Fig. 1) which were conspicuous by day 4 post-inoculation. At this point, there were not significant differences in abscess size between IA (19.5±0.5 mm^2), SHAM (20.7±2.5 mm^2) and VAG groups (20.7±2.1 mm^2); (Fig. 1D-F). The abscesses continued to grow in all groups, but by day 7 the size was almost double in the IA (32.7±2.5 mm^2) and SHAM groups (34.5±2.3 mm^2) when compared with VAG animals (18.3±3.5 mm^2) ($p<0.01$); (Fig. 1G-I). The comparison of the abscess size between the three groups can be seen in Fig. 1J.

This development was also examined microscopically. The inflammatory foci can be appreciated microscopically by H&E staining (Fig. 2), showing a large number of inflammatory cells in all three groups. The morphology of the inflammatory focus was similar in sizes at 12 h, in the three experimental groups (Fig. 2A-C) perhaps the number of inflammatory foci was mayor in VAG animals, thus, no differential histological changes between IA and SHAM were observed. In each group, necrotic areas could be clearly observed at day 4 and 7 (Fig. 2D-I) in combination with inflammatory cells.

Trophozoites, immunohistochemically stained (Fig. 3A), showed numerical differences over time. A larger number of these amoeboid figures were observed during the first 4 days of ALA development. At 6 and 12 h we observed differences in the number of *E. histolytica* trophozoites/mm^2, finding a higher quantity in the VAG group ($p<0.05$ at 6 and 12 h). The results at 6 h were IA (1±0.115), SHAM (1.04±1.9) and VAG (5.4±1.14), and at 12 h were IA (3.47±0.49), SHAM (4.13±0.961) and VAG (6.88±0.66) (Fig. 3B). No significant differences were observed at 24 h. On days 2 and 4, a greater

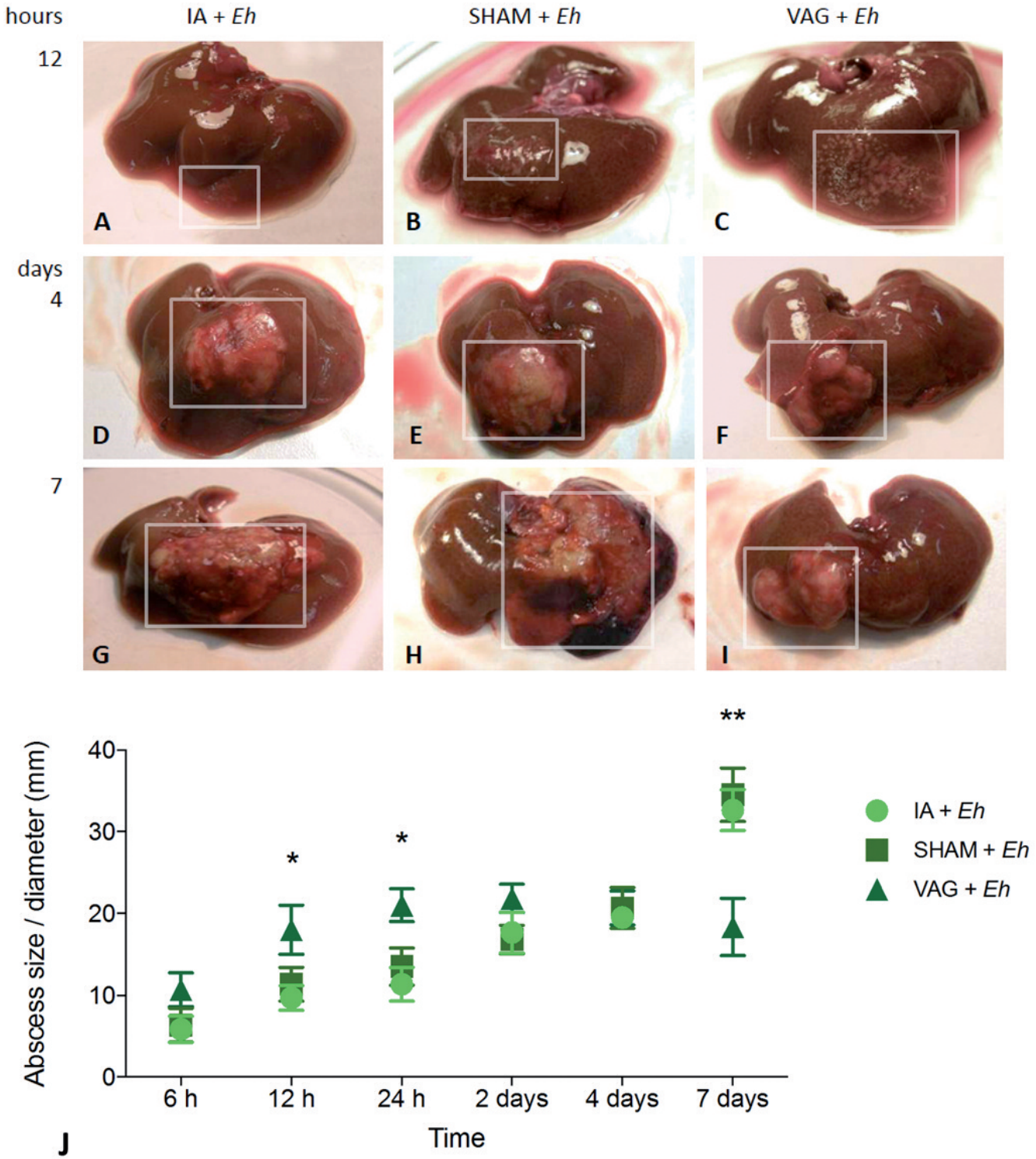

Fig. 1. Representative images of hamster livers removed at 12 h and day 4 and 7 in the IA, SHAM and VAG groups inoculated with *E. histolytica*. The animals used as a control (inoculated with CM only) are not shown. Note the development of ALA viewed macroscopically at each point of time (box), observing at 7 days **(I)** smaller abscesses in VAG hamsters compared to IA and SHAM animals. The mean ±SD (n=3) of the ALA size is shown for each of the IA, VAG and SHAM + Eh groups. *p<0.05, ** p<0.01 (1J).

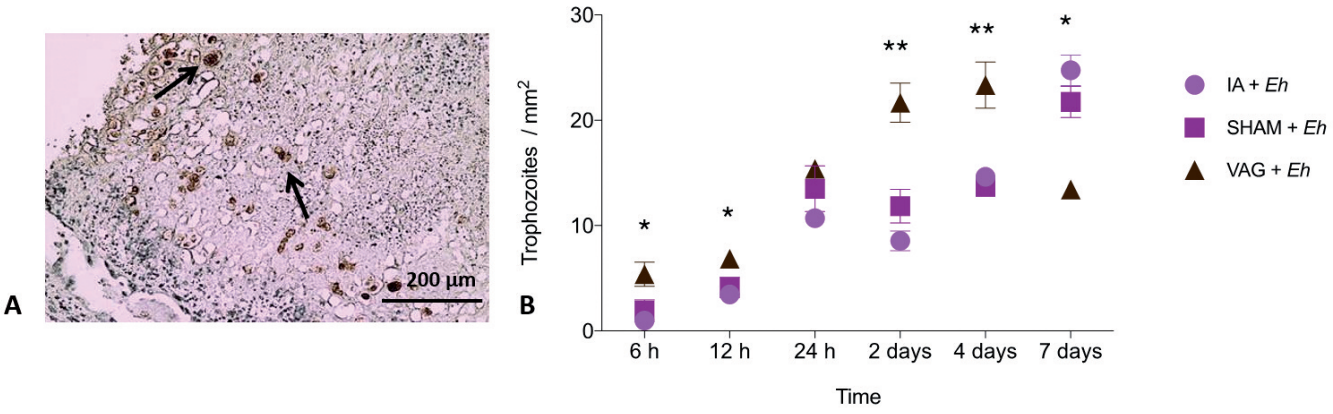

Fig. 3. Immunohistochemistry with anti-ameba shows the trophozoites of *E. histolytica* in brown (arrows) inside the inflammatory foci for the first 24 h post-inoculation **(A)**. The distribution and number of amoebae present per mm^2 was examined by immunohistochemistry, and counted by morphometry. The mean ±SD (n=3) is shown for each of the IA, VAG and SHAM + Eh groups. *p<0.05, ** p<0.01 **(B)**. For reasons of space, tissues inoculated with CM only are not shown.

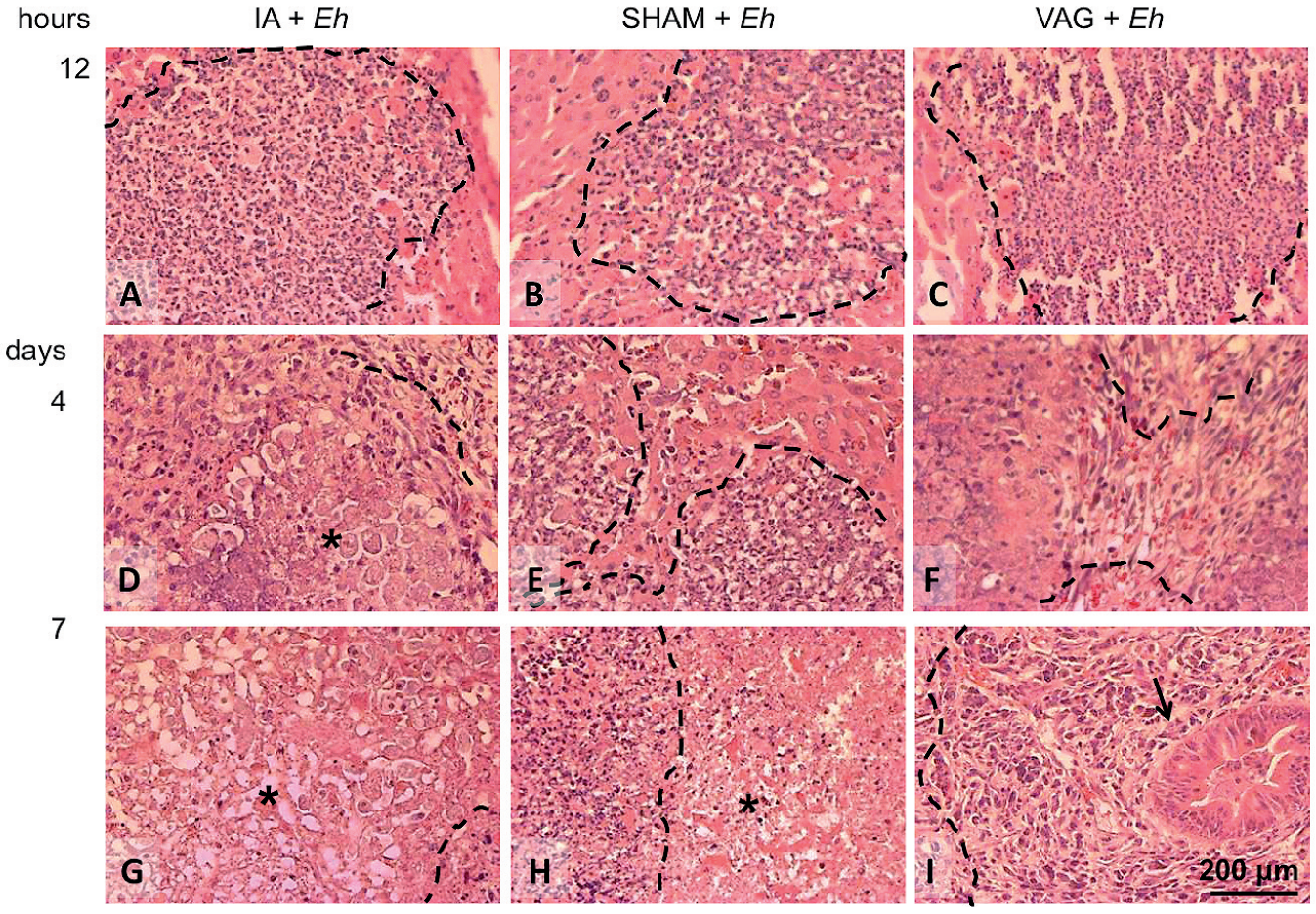

Fig. 2. H&E staining shows similar small areas of inflammation (interrupted lines) at 12 h post-inoculation (0.95±0.2 mm^2), which grow as time passes **(A-C).** After 4 and 7 post-inoculation, many areas of necrosis (asterisks) delimit the granulomas. Note the epithelioid cells (arrow) that form part of the granuloma in the VAG group **(I)**.

amount of trophozoites continued to be observed in VAG animals ($p<0.01$), while on day 7 the number of trophozoites was lower in VAG (13.43±0.87) than IA (24.73±1.45) and SHAM (21.73±1.48) ($p<0.05$), and this may be the reason why the abscess size decreased. It is important to mention that the AHA sections for all groups were performed at the same relative distance.

Collagen was identified microscopically after using Masson's trichrome stain (Fig. 4), analyzing tissue for all times studied and all animals inoculated with CM only (controls). The images 4A-C represent control hamsters, in some hepatic lobules, the collagen was observed slightly more in VAG animals on the 2nd day post CM inoculation shown in picture (Fig. 4C), but was not observed in all cases. The images displayed from day 4 and 7 post *E. histolytica* trophozoites inoculation (Fig. 4D-I) correspond to a production of collagen due to the ALA formation. In areas with necrotic tissue and fibrosis, the collagen was observed more clearly in VAG hamsters (Fig. 4F,I) compared to IA and SHAM animals especially in granulomas borders; due to the mix of collagen and inflammatory cells, the comparison of collagen through this method was qualitative exclusively since it allows to see the difference between the three experimental groups. The type of collagen was identified by Sirius Red staining. We observed mainly type I collagen in all three control groups inoculated with CM (Fig. 5A-C) as well as in the IA and SHAM groups inoculated with *E. histolytica* (Fig. 5D,E,G,H). This was not the case in the VAG + *E. histolytica* group, where there was a lower quantity of type I collagen and greater quantity of type III collagen (Fig. 5F,I), (Junqueira et al., 1978).

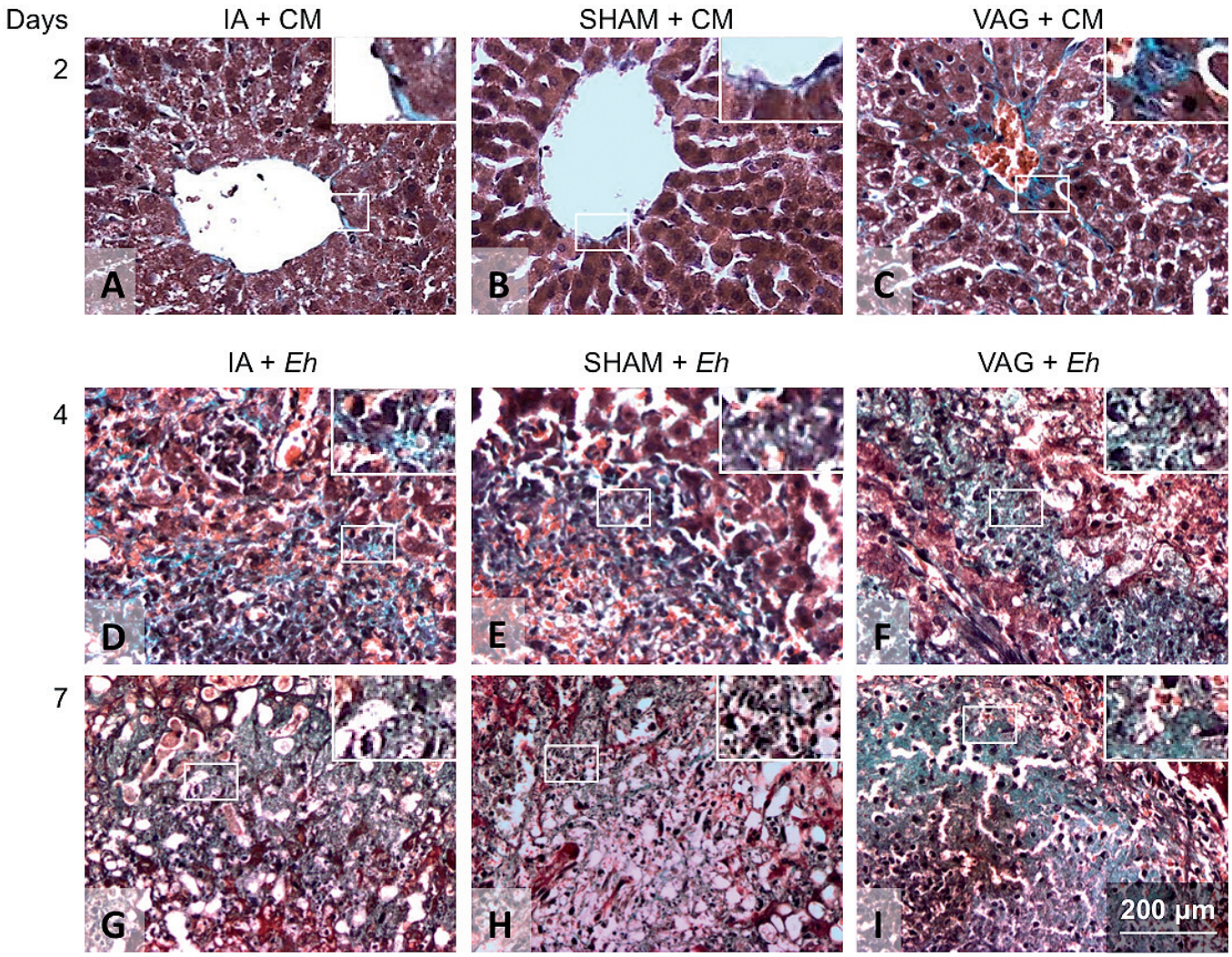

Fig. 4. Masson stain. **A-C.** Represent the IA, SHAM and VAG controls (inoculated with CM only) after day 2 post-inoculation (n=3). **D-I.** Represent days 4 and 7 post-inoculation for all experimental groups (inoculated with Eh). A larger amount of collagen was found on these days, thus facilitating a comparison of the three experimental groups.

Discussion

We herein show that a VAG can induce changes in the structure of the liver during the development of ALA. Previous studies have shown that up to day 7 post-inoculation, the VAG induces the deregulation of the inflammatory response during the development of ALA in hamsters, as well as causing some histological changes (Munoz-Ortega et al., 2011; Sanchez-Aleman et al., 2015). The present study describes for the first time the histopathological changes during the development of ALA from 6 to 7 days in vagotomized hamsters, taking in consideration the inflammatory cells that form the inflammatory foci, the necrosis and the number of trophozoites and the collagen that forms the fibrosis.

Several studies have focused on assessing different aspects of the development of ALA, including histological damage and fibrosis in the liver (Tsutsumi et al., 1984; Ventura-Juarez et al., 2002), cytokine production during the early stages (Pacheco-Yepez et al., 2011), the progress of treatments for chronic liver diseases (Wang and Hou, 2015) and the production of ALA with other species like *Entamoeba dispar* (Dolabella et al., 2012), but not in the way our vagotomy experimental model influences the ALA disease. Changes in the type of fibrosis have been evaluated in other organs, such as in the respiratory tract associated with asthma. In the latter case, the increase in type I and III collagen was found to be related to an elevated level of TGF-β in patients with inguinal hernia (Friedman et

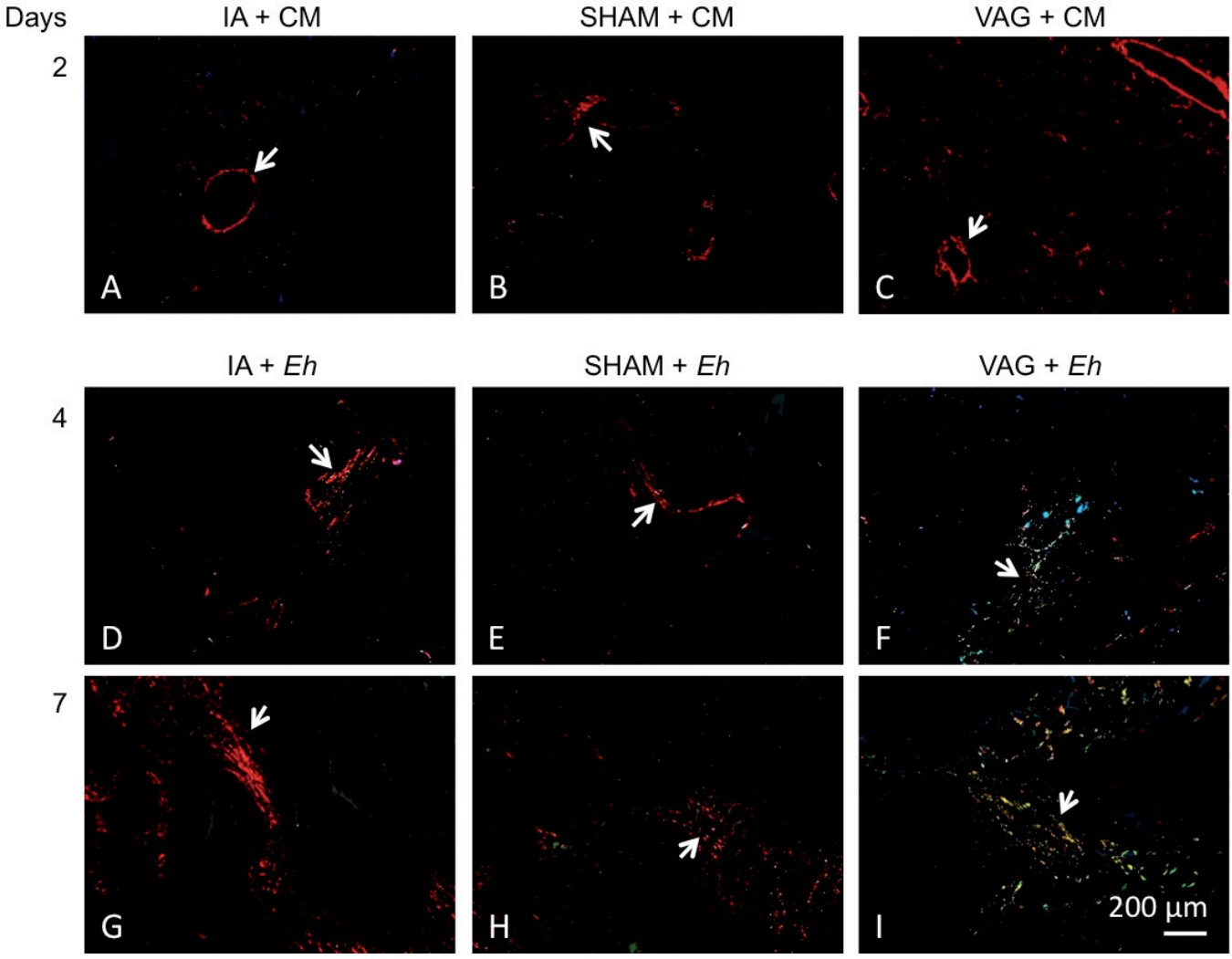

Fig. 5. Sirius Red Stain. **A-C.** Represent the IA, SHAM and VAG controls (inoculated with CM only) after day 2 post-inoculation (n=3). **D-I.** Represent days 4 and 7 post-inoculation for all experimental groups (inoculated with Eh). Red type I collagen is observed in all the animals inoculated with CM and the AI and SHAM + *E. histolytica* groups (arrows in **D, E, G, H)**. In VAG + *E. histolytica* groups, areas were observed with type III green and yellow type I collagen (arrows in **F, I**).

al., 1993; Chakir et al., 2003). Characterization of different liver diseases in experimental animals, such as fatty liver, hepatitis, fibrosis and cirrhosis, have demonstrated changes in liver morphology (Ye et al., 2004; Viladrich et al., 2008), but in this case, there are also structural differences in the experimental group compared with the controls.

Whereas potential benefits have been obtained by stimulating the VN in arthritis models, a vagotomy exacerbates the disease and stimulation with nicotine decreases it considerably (van Maanen et al., 2009), so the same happened with VN denervation in our experiment, but not until the 7th day of ALA formation, which indicates that maybe another kind of mechanism is activated by the animal model as in other studies related with VN denervation:the morphology of the aorta after a vagotomy in pigs reported that the amount of collagen and elastin was above normal (Sokolis et al., 2005). The effect of the VN in different body organs is not the same, for example, the influence of the VN on the neuroendocrine cell types is different in the small intestine than in the proximal colon. There was a decrease in chromogranin and somatostatin cells at 2 weeks after a vagotomy of the right VN, but the level of these cells returned to basal values at 8 weeks post-surgery. Serotonin cells were lesser in number at both 2 and 8 weeks post-surgery (Qian et al., 1999).

There are scant studies about the morphological changes that may occur in hepatic amoebiasis as a result of a vagotomy, or the potential impact of this procedure on the development of ALA. However, it has been observed that nAChRa7 stimulation attenuates collagen induction, which could help improve the development of the disease (van Maanen et al., 2009). The administration of glucocorticoids in the therapy related to Achilles tendon rupture in rats prevents maturation of tendon collagen fibers and decreases tendon strength (Taguchi et al., 2015). In the aforementioned studies, there were changes with the treatments. Nevertheless, no study has demonstrated how the absence of the VN induces the production of different types of collagen, or how the type of collagen is related to a greater activation of stellar cells or an increase in TGF-β (Munoz-Ortega et al., 2011; Sanchez-Aleman et al., 2015). There is no evidence that fibrosis may be involved in reducing the number of trophozoites, however, it is possible that the inflammatory response modified by subdiaphragmatic vagotomy may cause a decrease in the number of trophozoites or in the development of ALA.

The current contribution evaluated the induction exerted by the subdiaphragmatic vagotomy as well as the compensatory mechanisms of the organism in the face of the development of the disease. The interaction between the immune system and the parasympathetic nervous system somehow influences the development of the ALA (Sanchez-Aleman et al., 2015). Based on the present results, it can be seen that a vagotomy affects the development of ALA mainly in the first 24 h not only at the immune level but also in the histological structure of the abscess. Additionally, it can be said that the type of change in collagen affects the development of an abscess (e.g., whether or not it is diminished). A vagotomy produces a series of changes in the body that have been used since ancient times to produce positive effects in treatments, as against gastric ulcer (Sagatun et al., 2014) but on the other hand, it has seen that it can cause a Gastric intestinal metaplasia after a selective proximal vagotomy for the treatment of peptic ulcer (Rubio et al., 1993).

In the present study, a liver vagotomy influenced the histological structure of ALAs, the number of trophozoites present per square millimeter, and the production of collagen. It has been demonstrated that the parasympathetic nervous system not only interferes with the immune response, but also induces structural changes in the development of ALA. The comparison of tissues and the results concerning fibrosis confirm that the modification of collagen is a consequence of the absence of the VN in the liver. Changes in collagen may also have occurred because of increased levels of TGF-β, as has been reported recently (Sanchez-Aleman et al., 2015). Several studies have focused on assessing different aspects of the VN, including liver parenchymal abnormalities and the role of the VN in metabolism, the immune function related to systemic inflammatory responses and sepsis (Viladrich et al., 2008; Huston, 2012; Pavlov and Tracey, 2012; Boeckxstaens, 2013) and the activity and function of the VN on gut and the immune regulation (Matteoli and Boeckxstaens, 2013). Further studies are needed to explore the role of the VN in ALA in order to elucidate the mechanism by which this nerve plays a major role in the morphology of ALA. Based on previous studies and the insights presently attained, we conclude that the subdiapraghmatic vagotomy, which represents the absence of the parasympathetic nervous system, causes modifications in the morphological structure of hamster liver during the first 7 days of development of ALA with the intrahepatic inoculation of *E. histolytica* trophozoites, although the causes are not yet clear.

Acknowledgements. This work was supported by the National Council of Science and Technology (CONACYT-49749), and by the Autonomous University of Aguascalientes, Mexico (PIBB11-3). CONACYT fellowship No. 371793 was granted to Esperanza Sanchez-Aleman.

References

Aikat B.K., Bhusnurmath S.R., Pal A.K., Chhuttani P.N. and Datta D.V. (1979). The pathology and pathogenesis of fatal hepatic amoebiasis--a study based on 79 autopsy cases. Trans R. Soc. Trop. Med. Hyg. 73, 188-192.

Boeckxstaens G. (2013). The clinical importance of the anti-inflammatory vagovagal reflex. Handb. Clin. Neurol. 117, 119-134.

Borovikova L.V., Ivanova S., Zhang M., Yang H., Botchkina G.I., Watkins L.R., Wang H., Abumrad N., Eaton J.W. and Tracey K.J. (2000). Vagus nerve stimulation attenuates the systemic

inflammatory response to endotoxin. Nature 405, 458-462.

Chakir J., Shannon J., Molet S., Fukakusa M., Elias J., Laviolette M., Boulet L.P. and Hamid Q. (2003). Airway remodeling-associated mediators in moderate to severe asthma: Effect of steroids on TGF-beta, IL-11, IL-17, and type I and type III collagen expression. J. Allergy Clin. Immunol. 111, 1293-1298.

Davis A. and Pawlowski Z.S. (1985). Amoebiasis and its control. Bull World Health Organ. 63, 417-426.

Diamond L.S., Harlow D.R. and Cunnick C.C. (1978). A new medium for the axenic cultivation of entamoeba histolytica and other entamoeba. Trans. R. Soc. Trop. Med. Hyg. 72, 431-432.

Dolabella S.S., Serrano-Luna J., Navarro-Garcia F., Cerritos R., Ximenez C., Galvan-Moroyoqui J.M., Silva E.F., Tsutsumi V. and Shibayama M. (2012). Amoebic liver abscess production by entamoeba dispar. Ann. Hepatol. 11, 107-117.

Friedman D.W., Boyd C.D., Norton P., Greco R.S., Boyarsky A.H., Mackenzie J.W. and Deak S.B. (1993). Increases in type III collagen gene expression and protein synthesis in patients with inguinal hernias. Ann. Surg. 218, 754-760.

Henry T.R. (2002). Therapeutic mechanisms of vagus nerve stimulation. Neurology 59, S3-14.

Huston J.M. (2012). The vagus nerve and the inflammatory reflex: Wandering on a new treatment paradigm for systemic inflammation and sepsis. Surg. Infect. (Larchmt) 13, 187-193.

Junqueira L.C., Cossermelli W. and Brentani R. (1978). Differential staining of collagens type I, II and III by sirius red and polarization microscopy. Arch. Histol. Jpn. 41, 267-274.

Junqueira L.C., Montes G.S. and Sanchez E.M. (1982). The influence of tissue section thickness on the study of collagen by the picrosirius-polarization method. Histochemistry 74, 153-156.

Luna L.G. (1968). Manual of histologic staining methods, institute of pathology, armed forces, 3rd ed. N.Y.

Matteoli G. and Boeckxstaens G.E. (2013). The vagal innervation of the gut and immune homeostasis. Gut 62, 1214-1222.

Montes G.S. and Junqueira L.C. (1991). The use of the picrosirius-polarization method for the study of the biopathology of collagen. Mem. Inst. Oswaldo Cruz 86 (Suppl. 3), 1-11.

Mukhopadhyay M., Saha A.K., Sarkar A. and Mukherjee S. (2010). Amoebic liver abscess: Presentation and complications. Indian. J. Surg. 72, 37-41.

Mullan D.P. and Williams N.E. (1965). Left-sided amoebic liver abscess with pulmonary involvement, pericarditis, and pseudocholinesterase deficiency. Br. Med. J. 1, 235-236.

Munoz-Ortega M., Quintanar-Stephano A., Garcia Lorenzana M., Campos-Esparza M.R., Silva-Briano M., Adabache-Ortiz A., Campos-Rodriguez R., Rodriguez M.G. and Ventura-Juarez J. (2011). Modulation of amoebic hepatic abscess by the parasympathetic system. Parasite Immunol. 33, 65-72.

Otmishi P., Gordon J., El-Oshar S., Li H., Guardiola J., Saad M., Proctor M. and Yu J. (2008). Neuroimmune interaction in inflammatory diseases. Clin. Med. Circ Respirat. Pulm. Med. 2, 35-44.

Pacheco-Yepez J., Galvan-Moroyoqui J.M., Meza I., Tsutsumi V. and Shibayama M. (2011). Expression of cytokines and their regulation during amoebic liver abscess development. Parasite Immunol. 33, 56-64.

Pavlov V.A. and Tracey K.J. (2012). The vagus nerve and the inflammatory reflex--linking immunity and metabolism. Nat. Rev. Endocrinol. 8, 743-754.

Petri W.A. Jr, Haque R. and Mann B.J. (2002). The bittersweet interface of parasite and host: Lectin-carbohydrate interactions during human invasion by the parasite entamoeba histolytica. Annu. Rev. Microbiol. 56, 39-64.

Qian B.F., el-Salhy M., Danielsson A., Shalaby A. and Axelsson H. (1999). Changes in intestinal endocrine cells in the mouse after unilateral cervical vagotomy. Histol. Histopathol. 14, 453-460.

Ragland B.D., Ashley L.S., Vaux D.L. and Petri W.A. Jr (1994). *Entamoeba histolytica*: Target cells killed by trophozoites undergo dna fragmentation which is not blocked by bcl-2. Exp. Parasitol. 79, 460-467.

Rogers L. (1922). The lettsomian lectures on amoebic liver abscess: Delivered before the medical society of london. Br. Med. J. 1, 345-347.

Rubio C.A., Emas S., Slezak P., Nakano H. and Kalin B. (1993). Gastric intestinal metaplasia eleven years after randomized selective proximal vagotomy for peptic ulcer. Histol. Histopathol. 8, 243-245.

Sagatun L., Jianu C.S., Fossmark R., Marvik R., Nordrum I.S. and Waldum H.L. (2014). The gastric mucosa 25 years after proximal gastric vagotomy. Scand. J. Gastroenterol. 49, 1173-1180.

Salles J.M., Moraes L.A. and Salles M.C. (2003). Hepatic amebiasis. Braz J. Infect Dis. 7, 96-110.

Sanchez-Aleman E., Quintanar-Stephano A., Escobedo G., Campos-Esparza Mdel R., Campos-Rodriguez R. and Ventura-Juarez J. (2015). Vagotomy induces deregulation of the inflammatory response during the development of amoebic liver abscess in hamsters. Neuroimmunomodulation 22, 166-180.

Schmitz N., Laverty S., Kraus V.B. and Aigner T. (2010). Basic methods in histopathology of joint tissues. Osteoarthritis Cartilage 18 (Suppl. 3), S113-116.

Sierra-Puente R.E., Campos-Rodriguez R., Jarillo-Luna R.A., Munoz-Fernandez L., Rodriguez M.G., Munoz-Ortega M.H. and Ventura-Juarez J. (2009). Expression of immune modulator cytokines in human fulminant amoebic colitis. Parasite Immunol. 31, 384-391.

Sokolis D.P., Zarbis N., Dosios T., Papalouka V., Papadimitriou L., Boudoulas H. and Karayannacos P.E. (2005). Post-vagotomy mechanical characteristics and structure of the thoracic aortic wall. Ann. Biomed Eng. 33, 1504-1516.

Taguchi T., Kubota M., Saito M., Hattori H., Kimura T. and Marumo K. (2015). Quantitative and qualitative change of collagen of achilles tendons in rats with systemic administration of glucocorticoids. Foot Ankle Int.

Tanaka K., Ohkawa S., Nishino T., Niijima A. and Inoue S. (1987). Role of the hepatic branch of the vagus nerve in liver regeneration in rats. Am. J. Physiol. 253, G439-444.

Tsutsumi V., Mena-Lopez R., Anaya-Velazquez F. and Martinez-Palomo A. (1984). Cellular bases of experimental amebic liver abscess formation. Am. J. Pathol. 117, 81-91.

van Maanen M.A., Lebre M.C., van der Poll T., LaRosa G.J., Elbaum D., Vervoordeldonk M.J. and Tak P.P. (2009). Stimulation of nicotinic acetylcholine receptors attenuates collagen-induced arthritis in mice. Arthritis Rheum. 60, 114-122.

Ventura-Juarez J., Campos-Rodriguez R. and Tsutsumi V. (2002). Early interactions of *Entamoeba histolytica* trophozoites with parenchymal and inflammatory cells in the hamster liver: An immunocytochemical study. Can J. Microbiol. 48, 123-131.

Viladrich M., Sanchez O., Soley M. and Ramirez I. (2008). Alterations in liver parenchyma after sialoadenectomy in mice: Contribution of neutrophils and macrophages to the removal of damaged hepatocytes. Histol. Histopathol. 23, 1341-1352.

Wang Y. and Hou J.L. (2015). Current strategies for quantitating fibrosis in liver biopsy. Chin Med. J. (Engl) 128, 252-258.

Wang H., Yu M., Ochani M., Amella C.A., Tanovic M., Susarla S., Li J.H., Yang H., Ulloa L., Al-Abed Y., Czura C.J. and Tracey K.J. (2003). Nicotinic acetylcholine receptor alpha7 subunit is an essential regulator of inflammation. Nature 421, 384-388.

Ye X., Meeker H.C., Kozlowski P.B., Wegiel J., Wang K.C., Imaki H. and Carp R.I. (2004). Pathological changes in the liver of a senescence accelerated mouse strain (samp8): A mouse model for the study of liver diseases. Histol. Histopathol. 19, 1141-1151.

Accepted June 7, 2019